Electronic Supplementary Material (ESI) for Environmental Science: Atmospheres.

Supporting information for "Acoustic levitation with polarising optical microscopy (AL-POM): water uptake in a nanostructured atmospheric aerosol proxy"

S1. Image analysis

Images taken by the macroscope were processed using a *Python* script. The image was read-in and the levitated particles were defined by setting a threshold light intensity. Particles were easily defined due to the very low background light afforded by the polarising filters (see Fig. 1 – main text). The sum of the intensity for each droplet was calculated for each image taken during humidification. This was then normalised to the initial intensity value to form the experimental data presented in this study.

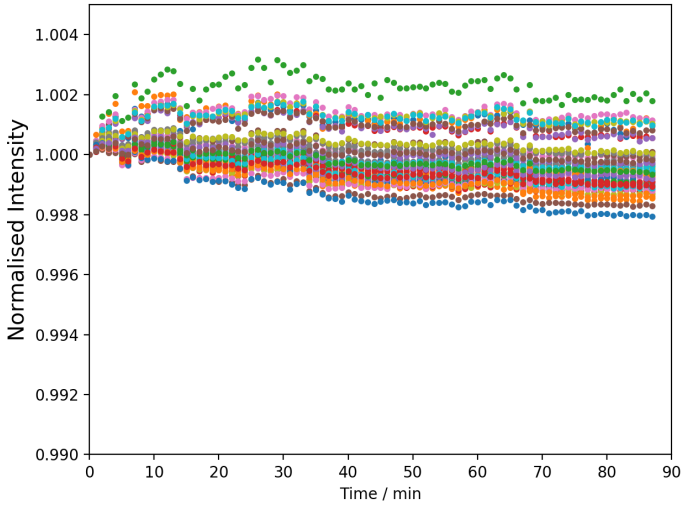

Figure S1. Normalised intensity vs time for 46 particles deposited simultaneously on a microscope slide. Data from each particle is represented by a different colour.

Uncertainty due to variations in the light source intensity was determined by nebulising the proxy sample and collecting 46 particles on a microscope slide. This microscope slide was placed inside the levitation-POM chamber and the intensity of each of these birefringent particles was measured for 89 min. We found that the light intensity for each particle varied on by *ca.* ± 0.15 % of the initial intensity. This was used as the absolute uncertainty associated with each experimental data point.

There seems to be a systematic increase or decrease in particle birefringence intensity depending on the particle measured. These variations are however very small and would have had little impact on the experimental data presented in the main text.

Particle size was determined by measuring the diameter of the particle in pixels, a graticule was used to calibrate the particle size in physical units (μm). Particles were 165 – 260 μm in diameter.

S2. Multi-layer water uptake model description

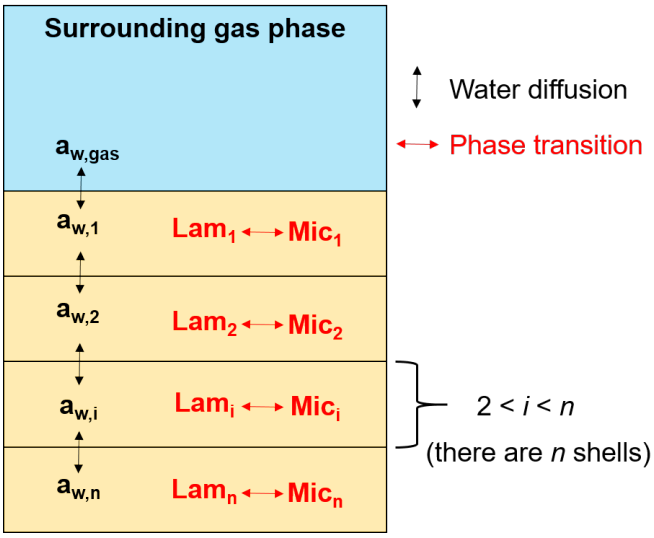

Figure S2. A schematic of the water uptake model created for this study. Water diffusion between the gas phase and particle layers is represented by the black arrows. Phase transition between the lamellar (Lam) and the close-packed inverse micellar (Mic) phase in each layer is represented by the red arrows. a_w is the water activity. There are n layers (shells) in the model.

Figure S2 describes the model, which accounts for: composition-dependent uptake and loss of water to and from the particle; composition-dependent diffusion of water between model layers and the surfactant phase transition from lamellar bilayer to close-packed inverse micelles.

The amount of water is represented as water activity (a_w) in the model. The use of a_w returned the best fits to the experimental data.

The spherical particle is split into a number (n) of layers. The amount of water in model layer i is described by eq. 1, where 1< i < n-1:

$$\frac{d(a_w)_i}{dt} = k_{b,b,w,i}\left(a_{w,i-1} - a_{w,i}\right)\frac{A_i}{V_i} + k_{b,b,w,i+1}\left(a_{w,i+1} - a_{w,i}\right)\frac{A_{i+1}}{V_i}$$

A_i is the surface area of layer i, V_i is the volume of shell i and $k_{b,b,w,i}$ is the rate of water transport within layer i. The core layer (n) only includes water transfer between this layer and layer n -1.

A relationship between $k_{b,b,w,I}$, water diffusivity (D_w) and layer thickness (δ) for each layer is given as per Shiraiwa et al.:

$$k_{b,b,w,i} = \frac{4D_{w,i}}{\pi\delta}$$

Water uptake and loss to and from the particle is accounted for in the first model layer:

$$\frac{d(a_w)_1}{dt} = k_{b,w,1}\left(a_{w,2} - a_{w,1}\right)\frac{A_2}{V_1} + \left(J_{abs} - J_{des}\right)\frac{A_1}{V_1}$$

This model accounts for differences in the rate of water uptake to the surface layer due to differences in water diffusivity that are expected between phases. Most notably, diffusion in

the lamellar phase is highly anisotropic and depends on the orientation of the lamellar planes.[1,2] We observed that the lamellae are highly oriented at the surface in this study. This difference is accounted for by introducing J_{abs} and J_{des}, which are the rate of water absorption and desorption, respectively:

$$J_{ads} = \{k_{a,lam}\, f_{lam,1} + k_{a,mic}\ (1 - f_{lam,1})\} \times (a_{w,gas} - a_{w,1})$$

$$J_{des} = -\{k_{d,lam} f_{lam,1} + k_{d,mic}\ (1 - f_{lam,1})\} \times (a_{w,1} - a_{w,gas})$$

J_{ads} and J_{des} incorporate the rate constant for water adsorption ($k_{a,lam}$ / $k_{a,mic}$) and loss ($k_{d,lam}$ / $k_{d,mic}$) for the lamellar and inverse micellar phases, respectively. The dependence on the amount of surface layer lamellar phase is accounted for by calculating the fraction of the lamellar phase in the first layer ($f_{lam,1}$). J_{ads} and J_{des} are also dependent on the a_w gradient between the first layer ($a_{w,1}$) and the gas phase ($a_{w,gas}$).

Phase change from the lamellar to the close-packed inverse micellar phase, observed for this system, is accounted for in the model. This was dependent on rate constants for micellar phase (k_{mic}) and lamellar phase (k_{lam}) formation and a_w in each layer:

$$\frac{d[Lam]_i}{dt} = k_{lam}[Mic]_i - k_{mic}[Lam]_i a_{w,i}$$

$$\frac{d[Mic]_i}{dt} = k_{mic}[Lam]_i a_{w,i} - k_{lam}[Mic]_i$$

The amount of lamellar ([*Lam*]) and (ordered) inverse micellar ([*Mic*]) phase in each layer is effectively their mass fraction. The model was initialised so that [*Lam*] = 100 and [*Mic*] = 0 in each layer. Written this way, the model maintains the total amount of self-assembled surfactant – *i.e.* [*Lam*] + [*Mic*] = 100. The assumption that no organic mass is lost is valid due to the low vapour pressure of oleic acid and sodium oleate.

k_{mic} was parameterised as a function of a_w in order to consider phase transition boundaries. We determined the lamellar-to-inverse micellar phase transition to start at ~ 55 % RH. Below this value, the following parameterisation was used to describe the steep decrease in lamellar-to-inverse micellar transition likelihood once a_w drops below phase transition water activity ($a_{w,trans}$).

$$k_{mic}\,(a_w) = k_{mic}\frac{(a_w)^p}{(a_{w,trans})^p} \quad , \quad where\ a_w < a_{w,trans}$$

p is a fitting parameter used during the optimisation process. $a_{w,trans}$ makes it possible to include other phase transitions in the model if other phase transitions are observed for a system.

S3. Scattering pattern from a randomly oriented lamellar phase

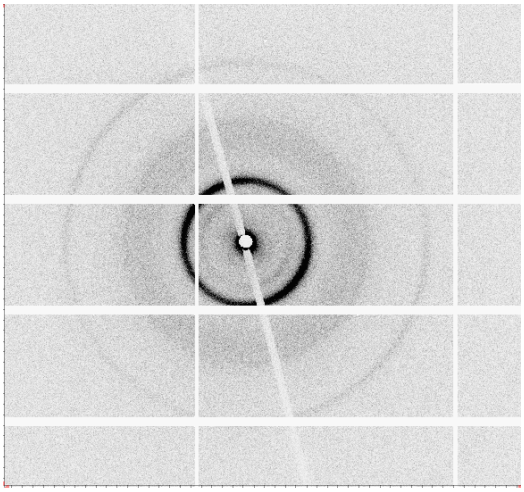

Figure S3. A 2-D SAXS pattern from the centre of a levitated oleic acid-sodium oleate particle at a 1:1 wt ratio. The intense inner scattering ring and outer two rings are consistent with the lamellar phase. There is no radial intensity variation for each ring, meaning this is an isotropic (randomly oriented) lamellar phase.

S4. Optimised model parameters

Model parameter	***Description***	***Optimised value (220 & 260 μm diameter particles)***	***Optimised value (165 & 190 μm diameter particles)***
$k_{a,lam}$	Rate of water absorption into the surface lamellar phase (s^{-1})	7.59×10^{-2}	8.06×10^{-2}
$k_{a,mic}$	Rate of water absorption into the surface close-packed inverse micellar phase (s^{-1})	3.81×10^{-1}	7.69×10^{-1}
$k_{d,lam}$	Rate of water loss from the surface lamellar phase (s^{-1})	3.50×10^{-3}	6.94×10^{-4}
$k_{d,mic}$	Rate of water loss from the surface close-packed inverse micellar phase (s^{-1})	7.03×10^{-3}	7.84×10^{-3}
k_{mic}	Rate of close-packed inverse micellar phase formation (s^{-1})	4.09×10^{-3}	6.48×10^{-3}
k_{lam}	Rate of lamellar phase formation (s^{-1})	1.96×10^{-3}	1.51×10^{-3}
$D_{w,lam}$	Diffusion coefficient of water through the lamellar phase ($cm^2\ s^{-1}$)	[2.79×10^{-9}]*	[3.08×10^{-9}]*
$D_{w,mic}$	Diffusion coefficient of water through the close-packed inverse micellar phase ($cm^2\ s^{-1}$)	[9.51×10^{-4}]*	[9.00×10^{-4}]*
p	Fitting parameter to account for the lamellar-to-close-packed inverse micellar phase boundary	9.97	9.88

Table S1. Model parameters varied during global optimisation. *Diffusion coefficients were converted from model values to physically meaningful values utilising $D_{w,mic}$ reported by Hendrikx *et al.* ($2.4 \times 10^{-8}\ cm^2\ s^{-1}$).[3]

S5. The levitation-polarising optical experiment with a webcam and higher resolution optics

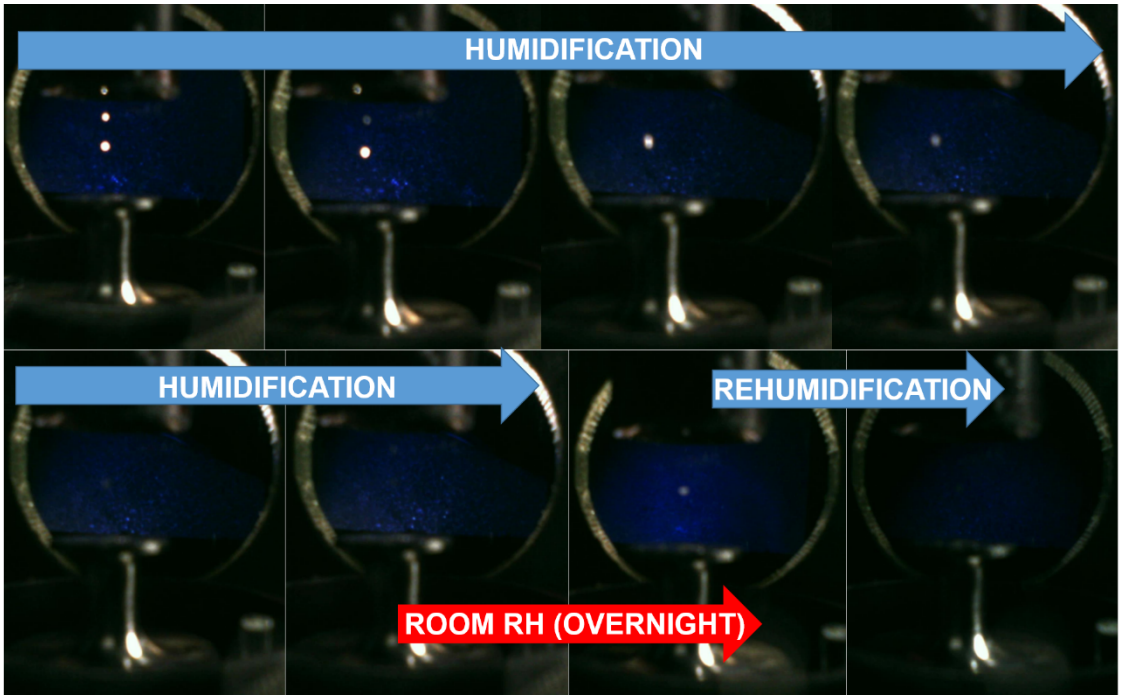

Figure S4. Images of an experiment carried out with the experimental setup described in this study, but with a webcam in place of the macroscope. 3 droplets are levitated and humidified. The birefringence of the particles decreased with continued exposure to 90 % RH. Focussing was not as optimal as was achieved with the macroscope. The upper two droplets were lost overnight, leaving one droplet remaining for rehumidification.

References

1 G. Lindblom and H. Wennerström, *Biophys. Chem.*, 1977, **6**, 167–171.

2 G. Lindblom and G. Orädd, *Prog. Nucl. Magn. Reson. Spectrosc.*, 1994, **26**, 483–515.

3 Y. Hendrikx, P. Sotta, J. M. Seddon, Y. Dutheillet and E. A. Bartle, *Liq. Cryst.*, 1994, **16**, 893–903.